# A Conceptual Model for the Influence of TUTT Cells on Tropical Cyclone Motion in the Northwest Pacific Ocean

JASON E. PATLA,* DUANE STEVENS, AND GARY M. BARNES

*Department of Meteorology, University of Hawaii at Manoa, Honolulu, Hawaii*

(Manuscript received 2 July 2008, in final form 2 April 2009)

ABSTRACT

Eleven (10 Pacific, 1 Atlantic) tropical cyclones (TCs), which include typhoons/hurricanes and tropical storms, are examined using the latest 40-yr ECMWF Re-Analysis (ERA-40) dataset and Joint Typhoon Warning Center (JTWC) best-track data to determine if and how tropical upper-tropospheric trough (TUTT) cells influence TC tracks. This type of interaction has led to rather large TC track forecast errors at 72 h (2000+ km) in the northwest Pacific and is often ignored or poorly forecast due to inadequate numerical model TUTT cell predictions. Ten selected cases out of the initial 25 potential Pacific cases exhibited a ''nonstandard'' TC track; a TUTT cell was the sole large-scale transient feature within 2000 km of the TC's center, and the TC intensity was $>17$ m s$^{-1}$. The circulations' separation distance, orientation, intensity, and TUTT cell's closed circulation size are critical characteristics in determining the likelihood of a TUTT cell influencing a TC track. Interactions occur at distances greater than 1700 km, continue for periods from 24 to 48 h, and occur 2–3 times per year in the NW Pacific.

Examination of the TC's tropospheric winds' deep layer mean (100–1000 hPa), and upper (100–500 hPa), middle (300–850 hPa), and lower (500–1000 hPa) layers, along with various quadrants of the upper layer, demonstrate a link between the TUTT cell's wind field and the nonstandard TC tracks. A conceptual model of how a TUTT cell can influence TC track is presented. The model provides decision-grade operational guidance for TC forecasters using pattern recognition scenarios. Application of the conceptual model at the JTWC is currently under way.

## 1. Introduction

The American Meteorological Society's *Glossary of Meteorology* (Glickman 2000) defines a tropical cyclone (TC) as ''the general term for a cyclone that originates over the tropical oceans. This term encompasses tropical depressions, tropical storms, hurricanes, and typhoons.'' Though some academics distinguish TCs as hurricanes/typhoons with a tropical storm as their weaker counterparts, this paper applies the AMS definition. Accurately forecasting TC track requires a better understanding of the interaction between the TC and its environment. Large-scale environmental features commonly associated with a TC's environment include the subtropical ridge, midlatitude troughs, other TCs, and transient highs. Upper-level cold-core lows embedded within a tropical upper-troposphere trough (TUTT), or TUTT cells, are environmental features also believed to influence TC motion and are of considerable interest in the northwest Pacific Ocean.

Our research investigated the influence of TUTT cells on TC motion in the northwest Pacific, an often ignored or poorly forecast interaction that has been only speculated to actually occur. We performed an observational case study in an attempt to determine how, when, and why TUTT cells influence TC motion and to delineate criteria for determining the likelihood and outcome of such an interaction. Our methods result in the first-ever operational guidance for TC forecasters to use during these interactions and, with a better understanding, could provide a foundation for future studies in other basins.

### a. The TUTT and TUTT cells

TUTTs are elongated, narrow, cyclonic shear zones (Whitfield and Lyons 1992) located in the northern and southern Pacific and Atlantic Oceans during the summer

* Current affiliation: U.S. Air Force Weather Agency, Asheville, North Carolina.

*Corresponding author address:* Jason E. Patla, 20 Arbor Meadow Ln., Asheville, NC 28805.
E-mail: patla@hawaii.edu

DOI: 10.1175/2009WAF2222181.1

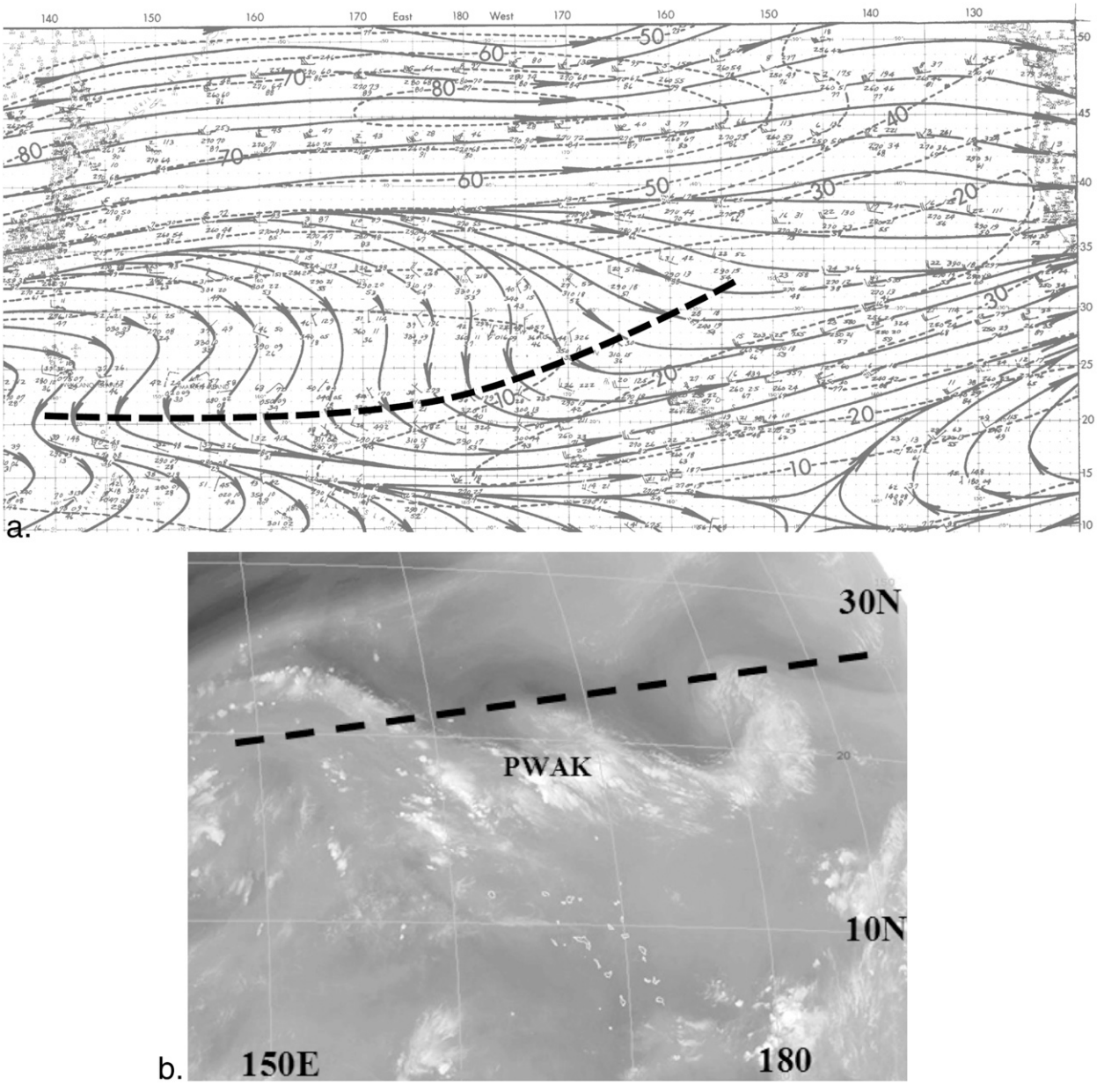


FIG. 1. (a) The average monthly climatological 200-hPa wind streamline (solid line) and isotachs (dotted line) for September over the North Pacific Ocean (Sadler 1975). The heavy dashed black line indicates the TUTT axis. (b) A *Multifunctional Transport Satellite-1R* (*MTSAT-1R*) image of a classic (though late season) TUTT across the central Pacific Ocean on 29 Oct 2007. Wake Island is annotated PWAK near the center of the image. The heavy dashed black line indicates the approximate TUTT axis.

months with peak intensity during July–September. The North Pacific TUTT, or midoceanic trough, is a semipermanent feature that extends east-northeast to west-southwest from ~35°N in the eastern Pacific to ~15°N in the western Pacific. The TUTT was first identified by Sadler (1967, 1975, 1976) on his monthly 200- and 300-hPa wind climatology as an induced trough between the boreal subtropical and subequatorial ridges that extend from eastern Asia and western North America, respectively. The TUTT appears as a smoothed depiction of the paths taken by transient TUTT cells but may also reflect the large-scale flow (Fig. 1a). An example of a well-formed TUTT using water vapor imagery is shown in Fig. 1b.

Colton (1973) and Thorncroft et al. (1993) suggested that upper-level circulations form within the TUTT due to barotropic instability associated with midlatitude troughs penetrating into the subtropics. Eddies eventually ''cut off'' from the trough and move as independent

circulations, which retrograde toward the west inside the TUTT (Kelly and Mock 1982). Similarly, eddy formation north of the subtropical jet provides another source of development. In general, though, there is no consensus on how TUTT cells form.

Composite analysis by both Kelly and Mock (1982) and Chen and Chou (1994) indicated that North Pacific TUTT cells generally track toward the west-southwest at ~4.3 m $s^{-1}$, approximately with the phase speed of Rossby waves. They have a mean wavelength of ~3000 km and a mean lifetime of about a week. Their circulation is typically confined between 100 to 600 hPa, with the strongest horizontal circulation near 200 hPa. At this level, the circulation's maximum horizontal winds are ~10 to ~20 m $s^{-1}$ at an average ~850 km radius. TUTT cell winds can also be enhanced if their circulation merges with the flow of other upper-level large-scale features. Chen and Chou (1994) found that most (87%) TUTT cells contain ''jet streaks'' (20–30 m $s^{-1}$) within their outer circulation either to the northwest or south of the centers in the North Pacific. These jet streaks correlated well with larger, more intense, and longer-lived TUTT cells. Winds along the southern periphery of the TUTT cell are generally strongest relative to the rest of the circulation primarily due to the cell's tendency to merge with strong upper-level (~150–300 hPa) westerlies.

### b. TUTT cell influence on tropical cyclone motion

There has been no previous observational or modeling research that directly addresses the influence of a TUTT cell on TC motion. This excludes effects resulting from a TC's change in intensity due to a TUTT's influence (e.g., Sadler 1976). The Joint Typhoon Warning Center (JTWC) has often referred to TC–TUTT cell ''interactions'' in their annual tropical cyclone reports (ATCRs) where TUTT cells caused a TC to slow down and/or move unexpectedly. Typically, no clear explanation of the TUTT cell's role is provided. The National Hurricane Center (NHC) has also made references to TC motion-related interactions with upper-level lows and has been more explicit in their discussions. Hurricane Erin, for example, was influenced by an upper-level low, which was regarded as the primary reason downtown Miami was spared a direct hit by the category 1 hurricane (Rappaport 2006).

### c. Tropical cyclone motion characteristics

TC motion ($M_{TC}$), defined here as the average vector displacement a TC moved between two 6-hourly JTWC best-track positions, can be divided into two primary components—TC translation ($T_{TC}$) and TC propagation ($P_{TC}$):

$$M_{TC} = T_{TC} + P_{TC}. \quad (1.1)$$

The components are distinguished by those processes influencing TC motion in a quiescent environment (propagation) and processes relying on the surrounding environmental flow (translation) (Fiorino and Elsberry 1989).

TC motion is mainly controlled by the environmental or ''steering'' flow associated with large-scale synoptic features, such as the subtropical ridge. The environmental steering flow is responsible for about 50%–80% of TC motion (Elsberry 1995) and, in some cases, up to ~90% (Neumann 1992). The steering layer that is most influential to TC motion is believed to be directly related to TC intensity (George and Gray 1976; Carr and Elsberry 1990; Wu and Kurihara 1996). A more intense TC (typhoon, hurricane) is expected to be steered by a deeper mean layer compared to a weaker TC (tropical storm, depression) due to the greater vertical extent associated with more intense TCs (Dong and Neumann 1986; Velden and Leslie 1991).

TC propagation occurs even if the background flow vanishes. The beta effect is typically the dominant TC propagation component and is due to the interaction between the TC's circulation and the earth's latitudinal planetary vorticity gradient. The TC's resultant $\beta$ drift is northwestward in the Northern Hemisphere (NH) at approximately 1–3 m $s^{-1}$ (Holland 1983). The $\beta$ drift is greater at higher latitudes and for TCs having a larger horizontal wind field. Other factors such as diabatic heating may also influence TC motion due to the asymmetric release of latent heat (Nolan et al. 2007). This, in turn, can modify the TC's potential vorticity (PV) distribution, which may affect TC motion (Fiorino and Elsberry 1989; Elsberry 1995).

### d. Binary tropical cyclone interaction

Fujiwhara (1923), Brand (1970), Dong and Neumann (1983), Lander and Holland (1993), and Carr and Elsberry (1998) have all discussed ''binary'' TC interaction characteristics. Their results yielded critical separation distances, interaction types (e.g., one way, mutual), and stages (e.g., approach, orbit, escape, and merger).

Lander and Holland's (1993, henceforth LH93) observational study focused on mutual TC interactions and between multiple ''TC scale vortices.'' LH93 cites but does not explicitly use ''mesoscale cyclones associated with TUTT cells'' as an example. LH93 focused on the independent tracks and movement of each circulation relative to an unweighted centroid (i.e., average coordinates on a Mercator projection) and described the motion characteristics. Their methods provide a good

framework within which to characterize TC–TUTT cell interactions.

### e. Operational justification and goals

Numerical forecast models are known for inaccurately projecting the location, structure, and intensity of TUTT cells. Fitzpatrick et al. (1995) described the Aviation Model's systematic bias in the Atlantic and the implications for TC genesis, track, and intensity forecasts. They speculated that the biases were most likely due to low spatial resolution, imperfect data, and the model physics. Similarly, Carr and Elsberry (2000a,b) discussed problems with the U.S Navy's Operational Global Atmospheric Prediction System (NOGAPS) in the northwest Pacific.

The JTWC has repeatedly identified problems with numerical model forecast TC track guidance in their ATCRs (JTWC 1994, 1996, 1998, 1999). According to the JTWC technical advisor, TC forecast models simply ''do not handle (TC) forecast tracks very well when a TUTT cell is involved'' (E. Fukada 2005, personal communication). Based on rather large track forecast errors (>2000 km) resulting from a lack of TC–TUTT cell interaction understanding and training, JTWC identified the need for research into these types of interactions and the development of operational guidance even though numerical models seem to have shown improvement over the past 5 yr. With this in mind, we plan on providing evidence of a TUTT cell's ability to influence TC motion and present an operational forecast guidance scheme in the form of a conceptual model designed to improve TC track forecasts.

## 2 Data and methodology

### a. Data

We utilized the latest (1975–2002) 40-yr European Centre for Medium-Range Weather Forecasts (ECMWF) Re-Analysis (ERA-40) 6-hourly dataset at near model resolution. The specific ERA-40 version was recreated by the National Center for Atmospheric Research (NCAR) and was transformed onto a $256 \times 128$ regular Gaussian grid at T85 spectral truncation ($\sim$1.406° or $\sim$156 km horizontal grid spacing) on 23 pressure levels. Various characteristics of each case (TUTT cell PV, relative vorticity, and circulation size) were analyzed using the aforementioned datasets.

To ensure a homogeneous ERA-40 database, TC case studies were constrained to 1994–2002. The JTWC ATCR and best-track data files were used as a reference for developing case studies and for 6-hourly TC surface locations and intensities. There were, however, no TUTT cell best-track datasets available. As a result, we used 200-hPa streamline analysis to approximately determine each circulation's center ($\pm$0.1° latitude–longitude) at the level of typical maximum intensity. TUTT cell intensity was determined by identifying the cell's maximum 200-hPa relative and potential vorticity. This created an independent TUTT cell ''best track'' dataset to match the much higher quality JTWC TC dataset.

### b. Methodology

#### 1) Case study identification and the definition of ''interaction''

The following criteria had to be met in order for a case to be selected. The primary goal of this selection was to have the most uncorrupted interactions possible in order to isolate the TUTT cell's influence on TC motion. The criteria included the following:

(i) *A nonstandard TC track was identified*, which indicated an irregular steering environment may have been present. Examples include ''stair step'' patterns, sudden or unexplained track deviations in speed and/or direction, and rare southward motion in the NH.

(ii) *A TUTT cell was in the vicinity (<2000 km or $\sim$18° latitude) of the TC near the time of the track deviation* and was a possible ''culprit'' in causing some of the TC's nonstandard motion. The 2000-km limit was based on the greatest published separation distance for binary TC interaction to occur ($\sim$1390 km) as identified by Brand (1970) plus an arbitrary 600-km buffer to account for the different scale/size between an average TUTT cell and TC.

(iii) *No other transient mesoscale or larger atmospheric features known to influence TC motion were observed within approximately 2000 km of the TC*. This criterion removed other likely causes for the TC's nonstandard track.

(iv) *The TC was at tropical storm strength or greater* (>17 m $s^{-1}$). This criterion was intended to ensure the TC had substantial vertical development (estimated core cyclonic wind field extended up higher than 500 hPa from the surface) to interact with a downward-extending TUTT cell and increase the likelihood of an interaction.

Twenty-five cases were initially reviewed after careful analysis of JTWC best tracks and satellite imagery during the period considered herein. Among all the cases available, only 10 were selected that fit all of the aforementioned criteria 24 h prior to and during the anticipated interaction period. As in LH93, for two TCs, the unweighted centroid-relative motions of the

TABLE 1. The final 13 ESLs (from the original 32) for each radial band utilized.

| Radial band (° lat) | Mass-weighted layer |
|---|---|
| 1–3 | Upper, middle, lower, DLM |
| 3–5 | Upper, middle, lower, DLM |
| 5–7 | Upper, middle, lower, DLM |
| Inner 7 | DLM |

TC (surface) and TUTT cell (200 hPa) for each case were analyzed to help determine the periods of potential mutual interaction between the two circulations. Interaction similarities between the TCs and TUTT cells were expected even though the circulations are obviously not on the same horizontal scale or of the same structure as the two TCs, nor did they have the fidelity of the two TC best tracks. The beginning of the interaction is identified and defined by a significant track change in the centroid-relative track near the beginning of each TC's nonstandard track. The midpoint between the two 6-hourly forecast steps that composed either side of the course change became the start point of the interaction period. The interaction end was then defined similarly by the two forecast steps, which compose the next centroid-relative track change and approximately corresponded with the end of the nonstandard track and/or the dissipation of the TUTT cell. The time between the start and end points was defined as the interaction period and the entire period as the interaction period ±~24 h.

### 2) FORECAST MODEL COMPARISON

Track errors for the official JTWC forecast, NOGAPS, and a climatology and persistence model (CLIPER) at 6-hourly intervals through 48–72 h were determined for each of the aforementioned 10 cases. Forecasters interpret the available guidance and create subjective forecasts based on a number of considerations, including a TC model's previous performance, applicable TC motion theory, proximity to major population centers or ports (sociopolitical), and forecaster workload and experience. Ideally, the JTWC forecast should exhibit the least error. This was not always the case, especially when a TUTT cell was nearby. NOGAPS (version 3.4) was a dynamic global spectral model in the horizontal (T159 spectral truncation, ~80 km in midlatitudes) and an energy-conserving finite difference model in the vertical [18 vertical levels before 1998, 24 levels afterward; Hogan et al. (2002)]. Virtually every source of data available to the ERA-40 reanalysis was also incorporated in the NOGAPS model runs. CLIPER is a 5-day statistical model that applies persistence from 12 h of previous TC track to the first 12 h of the forecast track. The model then considers the current TC location,

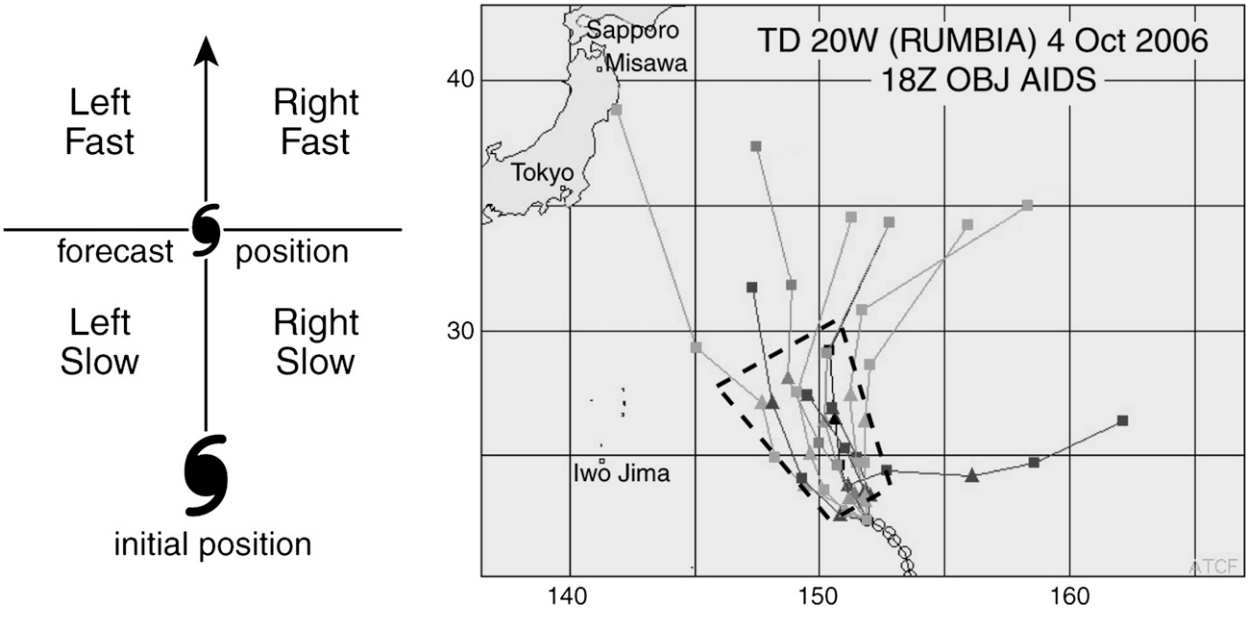


FIG. 2. (left) Potential TC motion bias (acceleration) resulting from a TUTT cell's influence on a TC's track. The orientation of the circulation ultimately determined the bias based on the flow of the TUTT cell overlapping the TC's steering environment. Assuming a straight initial forecast track, track biases to the left or right, faster or slower than forecast without consideration of the TUTT cell's contributing flow, were annotated. (right) A sample model ensemble is provided with a trapezoid field that indicates an estimated range of forecast TC motions for a set period and would encompass most of the forecast model track guidance.

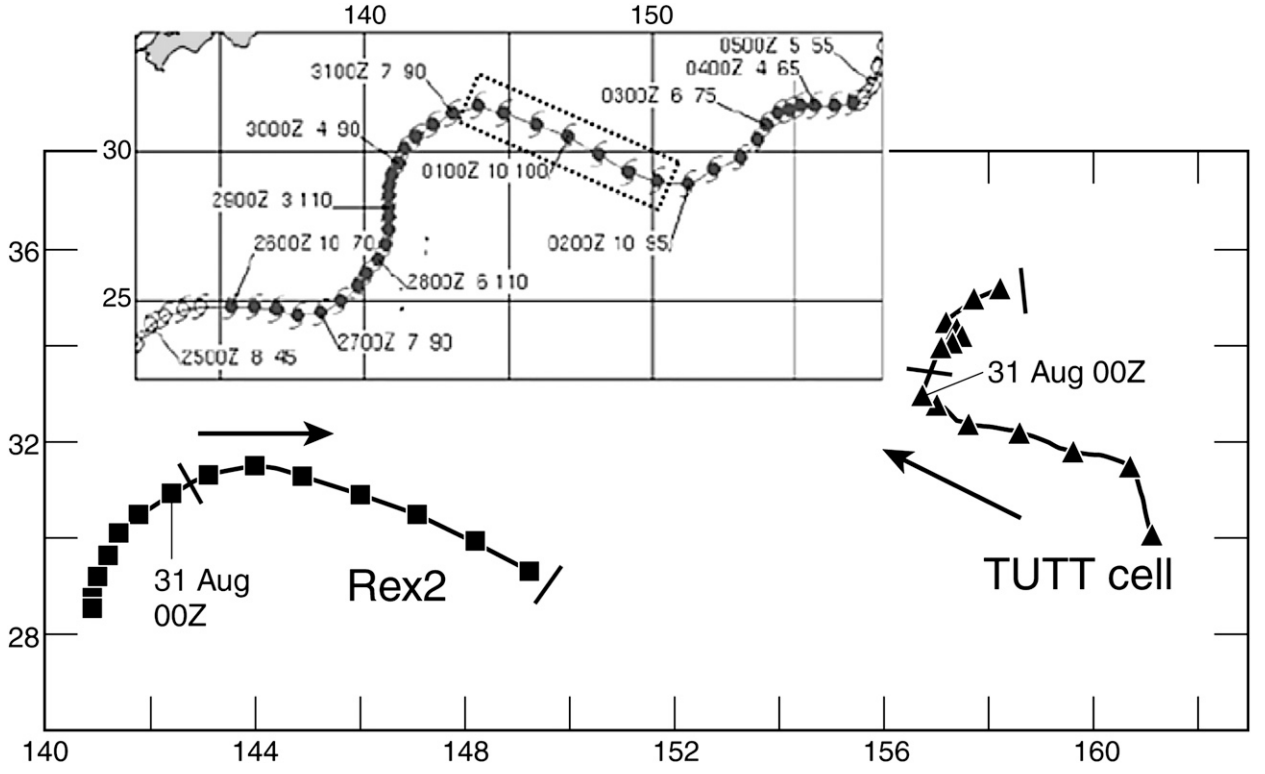


FIG. 3. A graphical depiction of both the TC (squares) and TUTT cell (triangles) tracks at 6-hourly intervals. The solid black arrow indicates the general direction of the TC motion. The approximate start (0000–0600 UTC 31 Aug 1998) and end (1800 UTC 1 Sep–0000 UTC 2 Sep 1998) points of the TUTT cell interaction period are annotated (solid lines). The end point was a result of the dissipation of a closed 200-hPa TUTT cell circulation. The inset graphic depicts the stair steps of Rex's (06W) track from the 1998 JTWC ATCR. The rectangular box roughly highlights the interaction period. Best-track intervals are 6 h. Annotation is in the form DDHH S WW, where DD is for the day of the month, HH is time in UTC hour), S is TC's forward speed (kt, 1 kt = 0.514 m $s^{-1}$), and WW is the TC's maximum 1-min-averaged sustained wind speed (kt).

intensity, motion vector, and Julian date to create a statistical forecast based on climatological TC paths with similar characteristics. CLIPER forecasts are considered a ''no skill'' output and are used as a baseline to show the value added by other forecast methods (Franklin 2006).

### 3) ENVIRONMENTAL STEERING LAYER IDENTIFICATION

There is a multitude of combinations of horizontal distances (degrees latitude radial bands around a TC's center, as defined by the JTWC best track) and vertical layer pairings that one could select to depict a TC's environmental wind field. We generically referred to all of these as environmental steering layers (ESLs). As a first guess, radial bands and layers demonstrated in previous studies to provide the best TC motion guidance were selected. Other ESL combinations (e.g., 400–700 hPa) were also considered for our preliminary analysis. Mean wind vectors for each ESL at every analysis time were compared to the track taken by the TC over the next 6 h, similar to what a forecaster would face (initial conditions versus after-the-fact analysis).

Sanders and Burpee (1968), Pike (1985), Dong and Neumann (1986), and Neumann (1979, 1992) applied mass weighting to the 10 standard-level winds from 100 to 1000 hPa. Their results indicated that this deep layer mean (DLM) provided the best representative wind field for short-term (≤24 h) forecasts. Chan and Gray (1982) utilized mass-weighted layer averages with various radial bands around TC centers in the northwest Pacific and statistically determined that the 5°–7° (556–778 km) radial band of the DLM flow correlated best with TC motion. Elsberry (1995) argued that the best ESL agreement with composite TC motion should be in the 1°–3° radial band, between 300–850 hPa. This pairing avoids most of the TC divergence and is in proximity to the TC's core.

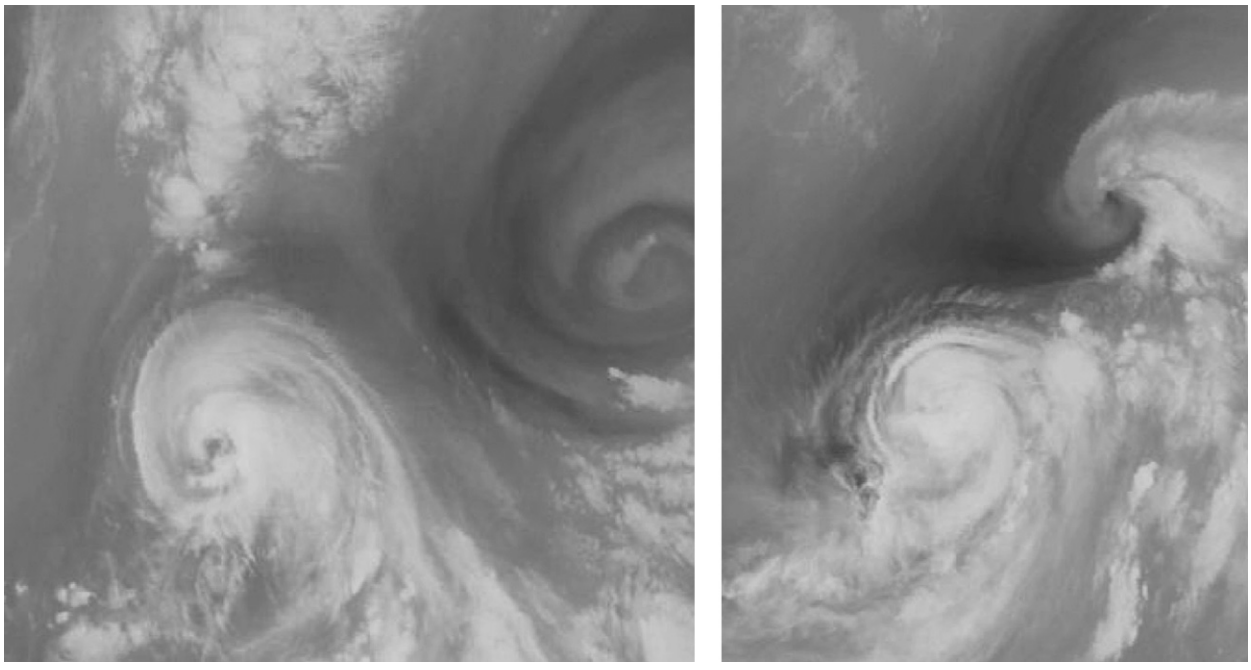

FIG. 4. *GMS-5* water vapor satellite imagery of Rex2 and a nearby TUTT cell at 0000 UTC 31 Aug 1998 (left) near the interaction start point and (right) just prior to the end of the TUTT cell interaction period at 1800 UTC 1 Sep 1998.

An upper (100–500 hPa) layer and a lower (500–1000 hPa) layer were analyzed as the layers expected to either include a TUTT cell's circulation or exclude it, respectively. The mass-weighted DLM then incorporated both layers. The middle layer consisted of mass-weighted winds between 300 and 850 hPa. Initially, 32 ESLs were analyzed but these were reduced to 13 after our preliminary analysis (Table 1).

#### 4) QUADRANT ANALYSIS

A TUTT cell was expected to modify only a portion of the TC's steering environment. To focus on the fractional contribution of a TUTT cell using a geographically fixed reference system, the TC's upper layer (100–500 hPa) was subdivided into quadrants (NE, NW, SE, and SW). Observing variations of each quadrant's mean wind value in a time series shows how the TC's upper layer responded to the TUTT cell winds. To identify evidence of a TUTT cell's influence on TC motion, we looked for a change in the mean/average wind flow of a fixed quadrant or quadrants nearest the TUTT cell that coincided with a change in TC motion. Quadrants not influenced by the TUTT cell's wind field were expected to remain relatively steady state.

TABLE 2a. Summary of all 10 cases' quantitative and qualitative metrics. The initial (subjective satellite based) and final (data evidence based) decisions of evidence existed that a TUTT cell influenced the TC's motion, the maximum depth of the TUTT cell's closed circulation down toward the surface, and the interaction start–end separation distances are provided in km.

| TC (year) | TC response to TUTT cell initial satellite-based estimate (evidence?) | TUTT cell closed-circulation depth (hPa) | Interaction separation distance at start (end) point (km) |
|---|---|---|---|
| Rex2 (1998) | Intense (yes) | <500 | 1340 (1050) |
| Babs (1998) | Intense (yes) | 600–700 | 1500 (1300) |
| Rex1 (1998) | Intense (yes) | 400–500 | 1700 (1360) |
| Ewiniar (2000) | Intense (yes) | 400–500 | 740 (790) |
| Bolaven (2000) | Moderate (yes) | 400–500 | 1500 (1300) |
| Amber (1997) | Weak (yes) | <300 | 680 (640) |
| Fred (1994) | Intense (no) | 500 to 600 | 1600 (1330) |
| Saomai (2000) | Moderate (no) | <300 | 1900 (1500) |
| Bart (1999) | Intense (no) | 250 to 300 | 1065 (765) |
| Polly (1995) | Weak (no) | <300 | 1650 (1200) |
| Erin (1995) | Moderate (yes) | 450 | 700 (450) |

TABLE 2b. Summary table of all 10 cases' quantitative and qualitative metrics. The TUTT cell's intensity at the interaction start point is listed in both maximum associated 200-hPa relative vorticity ($\zeta_r$) and potential vorticity (PV), and the TC's intensity range during the utilized periods. Here, $\zeta_r$ is in terms of $s^{-1}$.

| TC (year) | TUTT cell intensity max relative vorticity at the start point | TUTT cell intensity max PV at start point (PVU) | TC interaction intensity (m $s^{-1}$) |
|---|---|---|---|
| Rex2 (1998) | 1.50e-04 | 6 | 46–51 |
| Babs (1998) | 1.40e-04 | 4.5 | 21–39 |
| Rex1 (1998) | 1.20e-04 | 3 | 28–46 |
| Ewiniar (2000) | 2.60e-04 | 6.5 | 33–28 |
| Bolaven (2000) | 1.40e-04 | 3+ | 21–26 |
| Amber (1997) | 1.00e-04 | <2 | 26–33 |
| Fred (1994) | 1.70e-04 | 4 | 21–44 |
| Saomai (2000) | 1.00e-04 | <2 | 46–28 |
| Bart (1999) | 9.00e-05 | 2.5 | 67–51 |
| Polly (1995) | 5.00e-05 | <2 | 23–41 |
| Erin (1995) | 1.10e-04 | 4.3 | 27–34 |

A comparison between a TC's DLM with and without much of the TUTT cell's influence was accomplished by removing the quadrant of only the TC's upper layer (100–500 hPa) closest to the TUTT cell and re-creating the DLM. The new upper layer would then be composed of the remaining three quadrants while the lower layer (500–1000 hPa) remained unchanged. This was intended to show where the TC might have tracked without the TUTT cell's influence.

## 3. Results: Case studies

The 10 selected TC–TUTT cell cases were each initially identified using solely Geostationary Meteorological Satellite (GMS) infrared and water vapor imagery along with each TC's JTWC best track. The influence (e.g., change in direction and/or speed) a TUTT cell was believed to have exerted on a TC's track was noted based on the orientation of the two circulations. The TC's best-track motion was then compared to the JTWC and NOGAPS forecasts during the 24 h up to and including the interaction start point. This was then compared to an anticipated motion bias versus a typical ensemble forecast track (Fig. 2). Each TUTT cell, which either originated inside or moved into the TUTT, was subjectively labeled as having an ''intense,'' ''moderate,'' or ''weak'' appearance in satellite imagery.

Afterward, each of the 10 cases was analyzed (section 2b) to determine if there was an identifiable influence of the TUTT cell on TC motion. Evidence was primarily based on the vector difference between the TC's mass-weighted DLM and a newly computed DLM with the mass-weighted upper-layer quadrant closest to the TUTT cell removed. The following sections will discuss cases ''with'' and ''without'' evidence of a TUTT cell's influence on TC motion, a summary of all 10 cases, outlier cases, an example case from the Atlantic and the frequency of similar occurrences across the northwest Pacific basin. The TUTT cells associated with each of these cases originated within the climatological TUTT.

TABLE 2c. Summary table of all 10 cases' quantitative and qualitative metrics. The Forecast model performance (least and most error) and the approximate zonal (E–W) and meridional (N–S) extent of the TUTT cell's 200 hPa wind field based on the outermost closed isoheight at 10m intervals at the interaction start point are provided.

| TC (year) | Forecast model least (most) error | E–W (N–S) TUTT cell wind field at start point (km) |
|---|---|---|
| Rex2 (1998) | CLIPER (JTWC) | 920 (950) |
| Babs (1998) | JTWC (CLIPER) | 1600 (2180) |
| Rex1 (1998) | CLIPER (NOGAPS) | 1410 (1510) |
| Ewiniar (2000) | JTWC (CLIPER) | 800 (1350) |
| Bolaven (2000) | NOGAPS (CLIPER) | 1330 (1500) |
| Amber (1997) | CLIPER and JTWC (NOGAPS) | 1020 (630) |
| Fred (1994) | CLIPER (NOGAPS) | 1580 (1330) |
| Saomai (2000) | NOGAPS (CLIPER and JTWC) | 950 (1020) |
| Bart (1999) | NOGAPS (CLIPER and JTWC) | 550 (950) |
| Polly (1995) | NOGAPS (CLIPER) | 840 (600) |
| Erin (1995) | GFDL (CLIPER and AVNI) | 700 (540) |

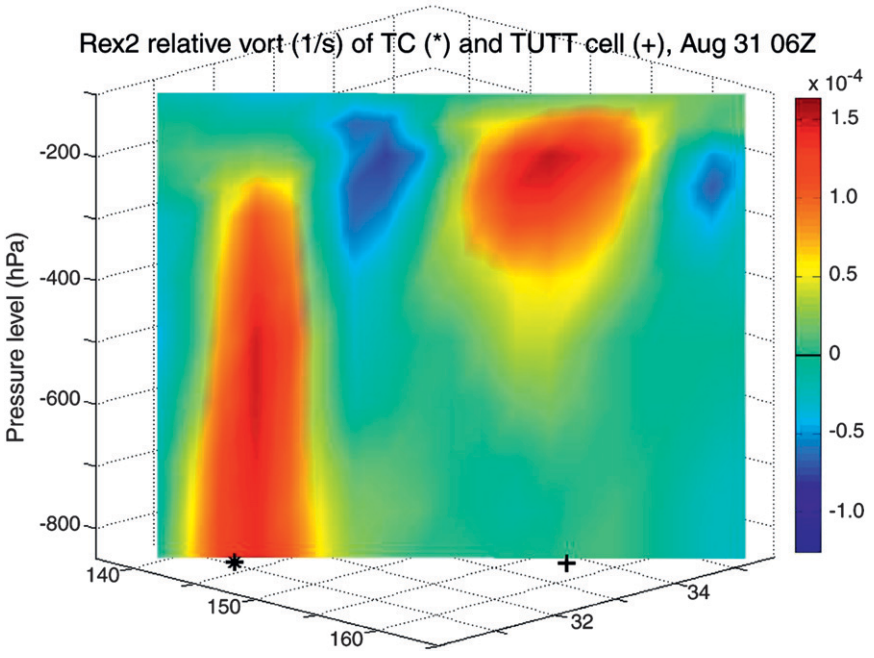


FIG. 5. Relative vorticity (image dependent, $10^{-4}$) cross section from 100 down to 850 hPa for Rex2 at 0600 UTC 31 Aug 1998 (near the interaction start point). Deeper yellow and red colors represent greater *positive* relative vorticity. Blues represent negative relative vorticity. The solid black line on the key represents $\zeta_r = 0$.

### *a. Case study showing evidence of a TUTT cell's influence on TC motion: Typhoon Rex(2) (06W) 1998*

According to the 1998 JTWC ATCR, ''the influence of three distinct TUTT cells caused Rex to deviate from its forecast northeastward track three separate times'' and was considered the ''paramount forecasting challenge'' of the year in the northwest Pacific. Rex was a long-lived TC with JTWC warnings from 24 August to 7 September. The TC tracked generally east-northeastward from the Philippine Sea (Fig. 3) and maintained typhoon

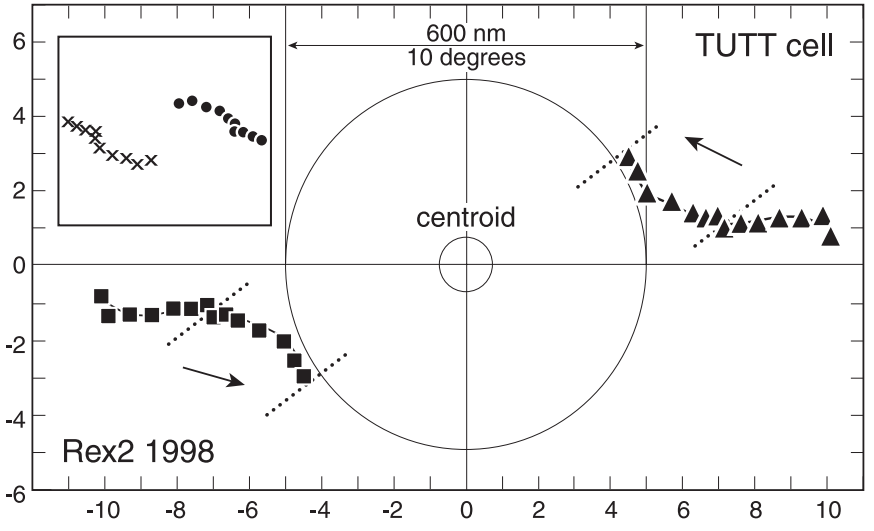


FIG. 6. Centroid-relative motion displayed using a two-point running average between Rex2 (squares) and the associated TUTT cell (triangles). The black dotted lines indicate the start (between 0000 and 0600 UTC 30 Aug 1998) and end (between 1800 UTC 1 Sep and 0000 UTC 2 Sep 1998) points of the TUTT cell interaction period. The black arrows indicate the general direction of motion. The inset (top left) is LH93's Polly and Rose (1974) centroid-relative motion.

intensity during each of the first two interactions, both of which were included in our case study. Each of Rex's three interactions was separated by at least a 36-h period and each is, therefore, handled as one of three independent cases. This discussion is about the second interaction—Rex2.

Rex2 was a strong TC (46–57 m $s^{-1}$) just prior to the interaction period as it tracked north at ~2 m $s^{-1}$ before a northeastward turn. The apex of the second stair step in the TC's track approximately coincides with the identified interaction ''start point'' between the TC and a broad and intense TUTT cell to the east-northeast. An infrared satellite loop shows an interaction that is reminiscent of Fujiwhara turning (i.e., mutual cyclonic rotation of two vortices; see Fig. 4), or the rotation of two cyclones around each other. The rotation ends with the two circulations oriented more north–south, filling of the TUTT cell, and a resumption of the TC's northeastward track. The orientation of the two circulations led to an expected increase in the TC's forward speed and a right (southward) cross-track bias (''right fast'' in Fig. 2).

Tables 2a and 2b list values taken for each case near the start of their interaction periods. The separation distance between the TC and TUTT cell at the start point was ~1340 km, which compares quite well with Brand's (1970) ~1390 km maximum distance for the onset of mutual cyclonic rotation between *two* TCs. Based on the ERA-40 reanalysis fields and compared to other cases, this TUTT cell was quite strong. At 200 hPa the cell had a maximum PV of 6 PVUs, a relative vorticity of $1.5 \times 10^{-4}$ $s^{-1}$, and a moderately broad diameter of ~1000 km based on the outermost closed 200-hPa isoheight. The circulation also extended down to lower than 500 hPa. Figure 5 provides a vertical cross section of the relative vorticity (100–850 hPa), approximately through the centers of circulation, which highlights the differences in intensity and depth between the TC and the TUTT cell. The start of the interaction, or start point, is identified by an abrupt change in the two circulation's centroid-relative motion between 0000 and 0600 UTC 31 August, which changed from a direct approach into a counterclockwise rotation, similar to LH93's Polly and Rose (1974) (Fig. 6). After this point, the TC turns toward the east, then southeastward while increasing its speed to ~5 m $s^{-1}$. This rare motion continues for ~42 h before the TC curves back toward the east then northeastward. The ''end point'' of the interaction is marked by the dissolving of the closed 200-hPa TUTT cell circulation from 1800 UTC 1 September to 0000 UTC 2 September.

All three forecasts used in this comparison [section 2b(2)] did very poorly during the 24 h leading up to and during the start of the interaction period. Errors ranged from 300 to over 2000 km at 72 h. Surprisingly, CLIPER performed the best overall. NOGAPS performs best for the first 12 h due to the model's initially slower forecast speeds compared to JTWC and CLIPER.

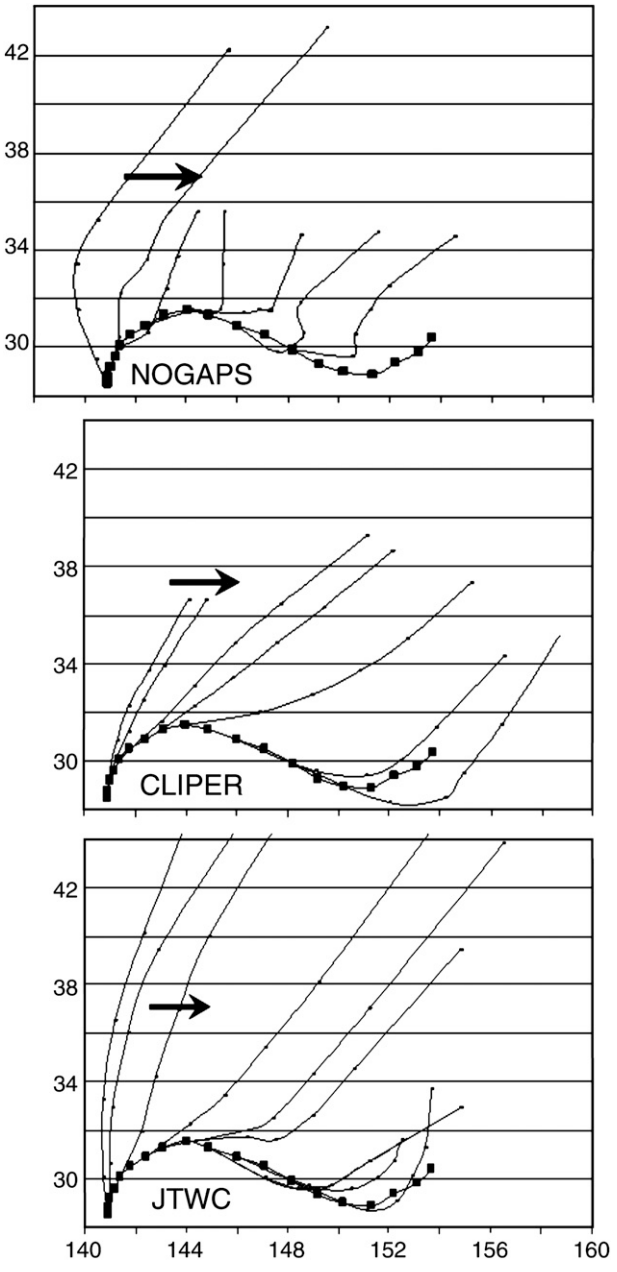


FIG. 7. Rex2 forecast tracks at 6- and 12-h intervals (varying) for (top left) NOGAPS, (top right) CLIPER, and (bottom) the JTWC. The black arrow indicates the general direction of the TC motion.

The center of the 200-hPa TUTT cell circulation remained in the region 30°–35°N, 156°–162°E, an area void of in situ upper-air observations and heavily reliant upon satellite observations for analysis. Considering the

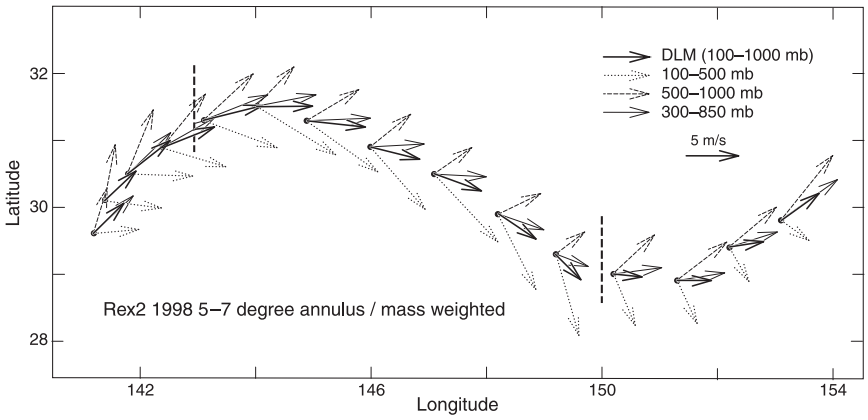


FIG. 8. Four-layer mean wind field analysis for Rex2. Mean vectors are scaled to the mean speed of the TC, which is equal to the distance between each 6-hourly time step. Vectors point in the mean radial direction for the 5°–7° radial band. Vertical dotted lines mark the interaction start (0000–0600 UTC 31 Aug 1998) and end points (1800 UTC 31 Aug–0000 UTC 1 Sep 1998).

lack of in situ data coupled with consistently sharp northward TC forecasts after only 12 h (Fig. 7), it is reasonable to expect that NOGAPS did not accurately forecast the TUTT cell's structure in terms of its intensity or depth as did the ERA-40 reanalysis. NOGAPS errors here exceeded 2000 km, which resulted in poor forecast guidance. CLIPER's reliance on persistence, conversely, allowed for a continuation of the storm's southeastward motion and a more subtle climatological turn back toward the northeast. This notably reduced CLIPER's long-range forecast errors.

The JTWC was initially concerned with a forecast that threatened Tokyo, Japan. The staff at the JTWC desired to maintain forecast persistence until they were confident the TC was not going to hit the port city. A distinct change in philosophy then occurred with the 1200 UTC 31 August forecast, after which errors drop significantly. No forecasts, however, indicated *any* southward motion until the TC had already curved southward after 0600 UTC 31 August (Fig. 7). This strongly suggests an underestimation of the TUTT cell's influence on TC motion by the JTWC operational numerical models. Even after the TC was moving southeastward, all except the JTWC forecast continued to show a quick return to an eastward then northward motion after only 12 h when, in fact, the TC tracked southeastward for ~2 days.

Figure 8 shows a time series of the mass-weighted mean wind vector for each of the four selected layers of the 5°–7° radial band (3°–5° and 1°–3° radial bands are not shown but had similar results). Based on this analysis, it is clear that the mean wind vector of the lower layer did not contribute to the TC's southward motion during the interaction period. Only the TUTT cell-influenced upper-layer mean wind vector yielded a significant increase of the southward component of motion followed by the middle and DLM layers 12–18 h into the interaction period. The overall speed of the TC was greater than all of the individual layers *except* the upper layer during this period. Outside the interaction period, the upper layer's mean flow was more zonal and with a notably reduced magnitude. But what caused the upper layer to exhibit such strong southward flow during this period?

Figure 9 shows a time series of the mean wind vector for the TC's upper layer subdivided into the geographically fixed quadrants. The two southern quadrants remained relatively unchanged with only a slight increase in magnitude toward the middle of the interaction period. The two northern quadrants both indicated a significant change from weak–northward or strong–northward to both strong–southward. The changes in the mean flow in the NE quadrant, however, led the NW quadrant by ~24 h. Figure 10 shows this is consistent with the time required for the TUTT cell's wind field to move from the NE into the NW quadrant where it merged with flow from an upper-level anticyclone ~14° to the west of Typhoon Rex. Regardless, Rex2 had already begun to move southeastward while only the NE quadrant had a strong southward component. This evidence implies that the TUTT cell significantly influenced the southeastward motion of the TC during this period.

Further evidence was provided by removing the TC's upper-layer quadrant closest to the TUTT cell and creating a hypothetical ''TUTT cell free'' DLM. Figure 11 shows a time series of the original mass-weighted DLM vector and this new DLM. Notice that the 5°–7° radial band of the new DLM vector exhibits a ~35% less magnitude than the original DLM and, most importantly,

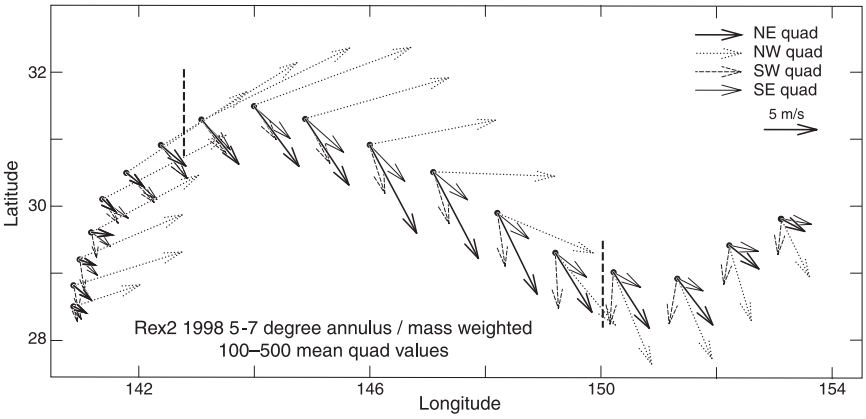


FIG. 9. Four-quadrant mean wind field analysis of the upper layer for Rex2. Mean vectors are scaled to the mean speed of the TC, which is equal to the distance between each 6-hourly time step. Vectors point in the mean radial direction for the 5°–7° radial band. Vertical dotted lines mark the interaction start (0000–0600 UTC 31 Aug 1998) and end points (1800 UTC 31 Aug–0000 UTC 1 Sep 1998).

no southward component during the interaction period. Without the TUTT cell, the TC would have taken a more east to east-northeastward track and been much closer to the JTWC and NOGAPS predictions, hence further supporting the inability of the current operational models at JTWC to predict TUTT cell interactions with TCs.

The environmental winds of the two northern quadrants did, interestingly, remain relatively strong and southward for 6–12 h *after* the interaction with the end point. Note, though, that the end of the interaction period was marked with the dissipation of the TUTT cell's *closed* 200-hPa circulation. A very sharp trough combined with the anticyclone to the TC's west *remained* for another 6–12 h (Fig. 12). This provided modest but weakening southward flow in the upper layer. Analysis of the four layers (Fig. 8) also indicated the lower layer (500–1000 hPa) simultaneously doubled in magnitude toward the northeast. This strengthening lower layer dominated the environmental flow, resulting in a DLM change and a turn in the TC's track.

### b. *Tropical Storm Babs and Typhoon Rex(2): Contrasting responses to TUTT cell interactions*

Rex2 and Babs had similar separation distances and TUTT cell characteristics but very different intensities. During their interaction periods, Rex2 was a strong

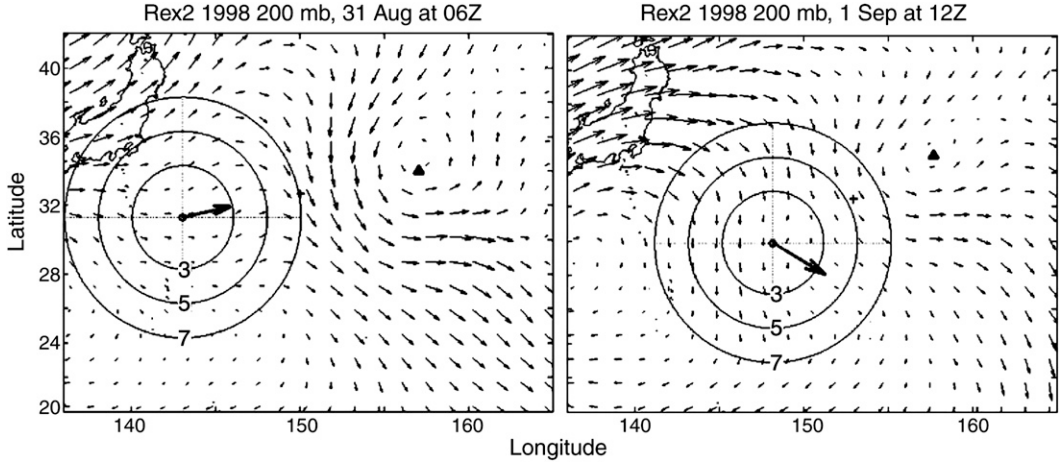


FIG. 10. Rex2 200-hPa wind field analysis at (left) 0600 UTC 31 Aug 1998 (near the interaction start point while moving at ~4 m $s^{-1}$) and (right) 1200 UTC 1 Sep 1998 (late into the interaction period and moving at ~6 m $s^{-1}$). The lowercase letter ''o'' represents the best-track low-level center of Rex2. The plus sign represents the centroid of the two circulations. The solid triangle represents the approximate 200-hPa TUTT cell circulation center. The closed circles represent the approximate 3°, 5°, and 7° radii, respectively, and are divided into quadrants. The solid black arrow represents the TC's trajectory.

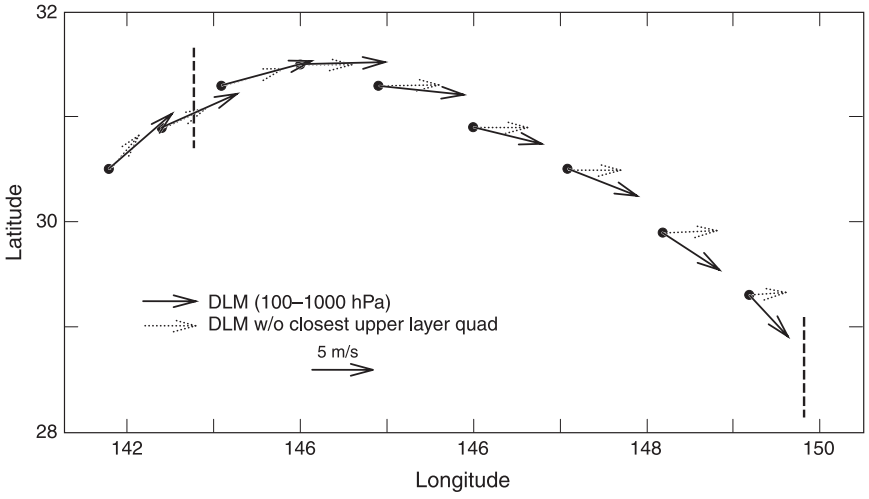


FIG. 11. The original 5°–7° radial band mass-weighted DLM (solid) and the new mass-weighted DLM with the upper-layer quadrant closest to the TUTT cell removed (dotted) for Rex2. Mean vectors are scaled to the mean speed of the TC, which is equal to the distance between each 6-hourly time step. Dashed vertical lines mark the interaction start (0000–0600 UTC 31 Aug 1998) and end points (1800 UTC 31 Aug–0000 UTC 1 Sep 1998). The TC track stops at the interaction end point as the TUTT cell's 200-hPa circulation center dissipates.

typhoon (~50 m $s^{-1}$) while Babs was only a moderate tropical storm (~25 m $s^{-1}$). Rex2 responded promptly to the radical changes in upper-layer flow (turned and increased speed to ~6 m $s^{-1}$) while Babs's response was much less apparent (gradual 1–2 m $s^{-1}$ turn). Had Babs been more intense under the same conditions, a greater response might have occurred. More intense TCs have a stronger circulation aloft, allowing for more interaction with a TUTT cell (Dong and Neumann 1986; Velden and Leslie 1991). Based on the inertial stability argument made by Holland (1983), we might expect a stronger TC to react throughout its entire column while a weaker TC may be distorted by changing upper-level winds. Figure 13 shows meridional cross sections of each circulation's relative vorticity field ($\zeta_r = 5 \times 10^{-5}$ $s^{-1}$ highlighted) near each case's respective interaction start point. In this comparison, Rex2 was the more intense and well-developed of the two TCs and had greater inertial resistance to horizontal shearing–displacement from the TUTT cell winds. TS Babs, on the other hand, was a weak and less developed TC with less resistance to vertical shearing.

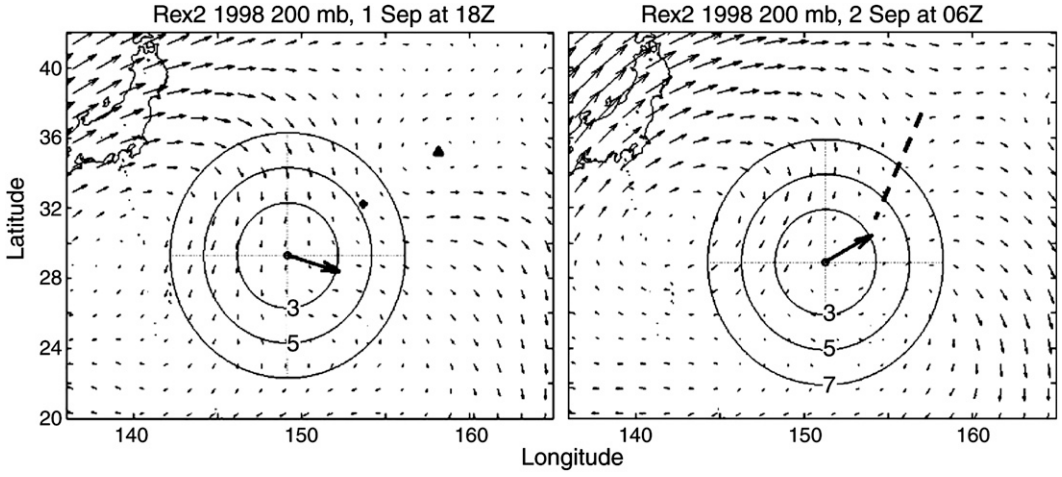


FIG. 12. As in Fig. 10 but at (left) 1800 UTC 1 Sep 1998 (near interaction end point and moving at 6 m $s^{-1}$) and (right) 0600 UTC 2 Sep 1998 (after interaction end point and moving at 5 m $s^{-1}$). The dashed line (right) represents the trough axis from the dissipated TUTT cell.

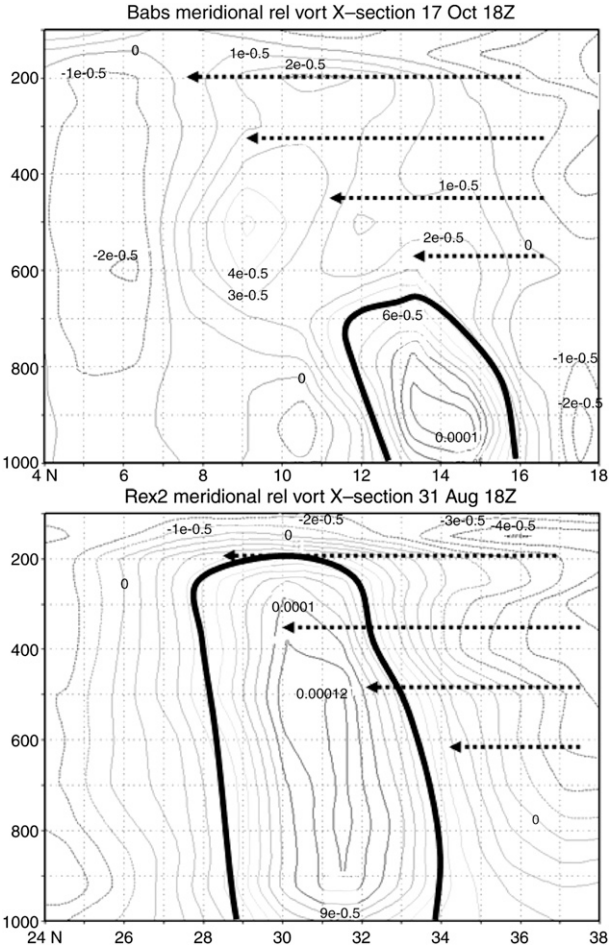


FIG. 13. Meridional vertical cross sections of the relative vorticity for (top) Babs (a 25 m $s^{-1}$ TC) and (bottom) Rex2 (a 50 m $s^{-1}$ TC) near their respective interaction start points. Approximate TUTT cell-induced upper-layer winds are superimposed with black dotted arrows. The $5 \times 10^{-5}$ $s^{-1}$ values of the relative vorticity are emboldened in black for both profiles. The TUTT cell characteristics for each case were very similar. Notice the dissimilar structure between the two TCs, including Babs's lack of vertical extent and greater downshear tilt compared to Rex2.

The lower half of its circulation responded slowly to the southward shear in the upper half and lagged behind compared to Typhoon Rex2, which moved as a solid-body vortex.

### c. *Example of a TUTT cell not influencing TC motion: Typhoon Bart (24W) 1999*

Bart formed in the central Philippine Sea east of Taiwan. It was during its final northward advance that a TUTT cell moved to the TC's east. The two vortices then moved in tandem to the north. The TUTT cell appeared large and intense in water vapor imagery (Fig. 14), but TUTT cell structure analysis revealed a perfect example of misleading satellite imagery.

Bart was an intense typhoon (>50 m $s^{-1}$) during the entire period. The ERA-40 reanalysis (Tables 2a and 2b) revealed that the TUTT cell had low values of PV (2.5 PVUs), weak relative vorticity ($\zeta_r = 9 \times 10^{-5}$ $s^{-1}$), a depth extending only to ~300 hPa, and a narrow closed circulation. We regard this TUTT cell as ''weak'' compared to the situations presented in sections 3a and 3b. Figure 15 shows the vertical cross section of the relative vorticity during the interaction period. The shallowness of the TUTT cell compared to Bart is obvious. The separation distance at the start point was ~1065 km and remained within this distance until the TUTT cell dissipated. Based on the orientation of the two circulations, we expected the TC to slow and turn eastward (''right slow'' in Fig. 2).

NOGAPS forecasts performed best followed by JTWC and CLIPER (errors of 190–900 km at 72 h). Climatologically, TCs in this area typically accelerate toward the northeast after recurvature versus Typhoon Bart's slow motion. This same initial slow motion and uncertainty over the timing of the TC's northeastward acceleration resulted in much of the JTWC forecast error. With the TUTT cell nearly due east of the TC, northerly flow on the TUTT cell's western periphery was expected to impinge on the TC's environment. This meridional contribution would be expected to turn the TC southward or slow its northward progression.

Vector time series for all layers, especially the upper layer, provide no clear evidence of southward flow during the TUTT cell interaction. The upper-layer flow was consistently to the east/right of and of similar magnitude (±1 m $s^{-1}$) to the TC's motion. A small eastward bias was also expected as winds around the southern periphery of the TUTT cell turned toward the east. However, no such bias was found. Analysis of Bart's 200-hPa wind fields indicated that the flow associated with the TUTT cell barely extended to within 5° of the TC center even though its separation distance was closer than many other cases. The TUTT cell's shallow circulation could not produce an identifiable influence on the TC's upper layer.

Figure 16 shows the original mass-weighted DLM vector and the new DLM vectors with the TC's upper-layer quadrant closest to the TUTT cell removed. Before the start point, both the original and new DLMs were similar. During the interaction, however, the new DLM had a reduced southerly wind magnitude (~10%–40%). This indicates that the TUTT cell failed to produce a mean northerly component within the TC's upper layer. Furthermore, the TC would have tracked even more slowly toward the north without the closest quadrant's (including the TUTT cell's winds) contribution to the upper layer.

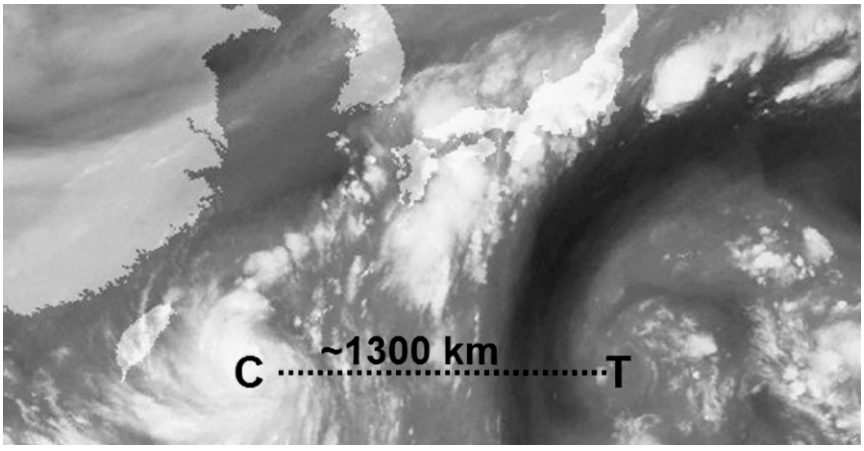


FIG. 14. *GMS-5* water vapor imagery for 0600 UTC 21 Sep 1999, about 12 h prior to the interaction start point. The capital letter T represents the approximate 200-hPa TUTT cell center and the capital C the center of Bart (57 m $s^{-1}$ intensity). The distance between the two circulations was approximately 1300 km.

### *d. Summary of all 10 Pacific cases*

Tables 2a–c provide a summary of each TC and TUTT cell characteristic. Cases were parsed between those showing evidence of a TUTT cell's influence on TC motion based on our methods and those that did not. Most TUTT cell characteristics fit quite well into these two groups except for one outlier in each group: Amber and Fred (Fig. 17). These will be discussed further in section 3e.

Comparing the two groups against our initial subjective satellite-only assessment revealed that 4 of our 10 initial estimates were incorrect. One case appeared to have a weak TUTT cell yet provides evidence of its influence on the TC's motion (Amber). Three other cases (Bart, Fred, and Saomai), conversely, had moderate- or intense-looking TUTT cells expected to cause some influence, but did not. These results emphasize the need for forecasters to have a quantitative estimate of TUTT cell winds, vorticity, and depth in addition to satellite imagery.

Interaction periods ranged from ~24 to ~48 h with an average of ~30 to ~36 h. Separation distances at the interaction start point varied from ~680 to ~1700 km

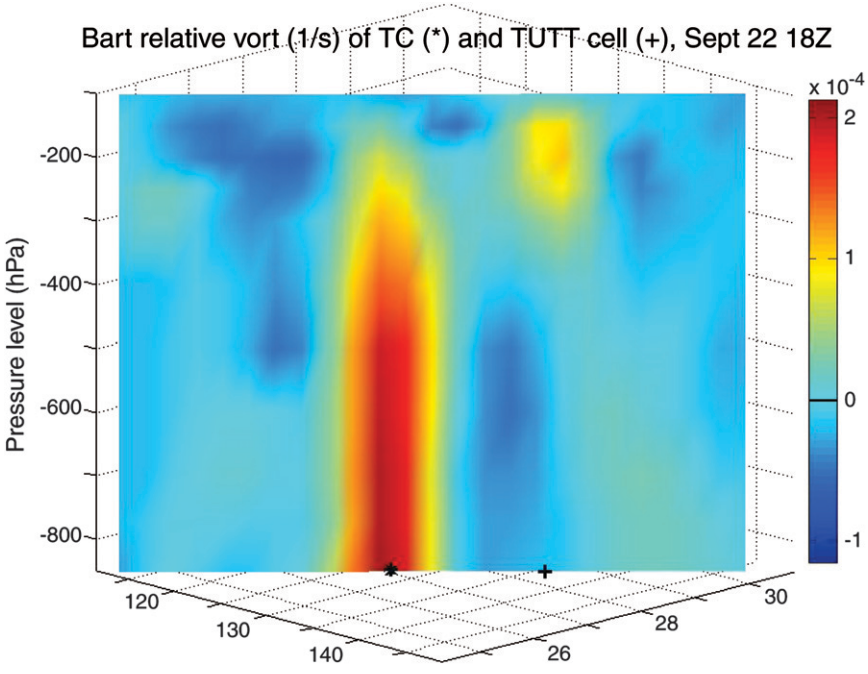


FIG. 15. As in Fig. 5 but for Bart at 1800 UTC 22 Sep 1999, just within the interaction period.

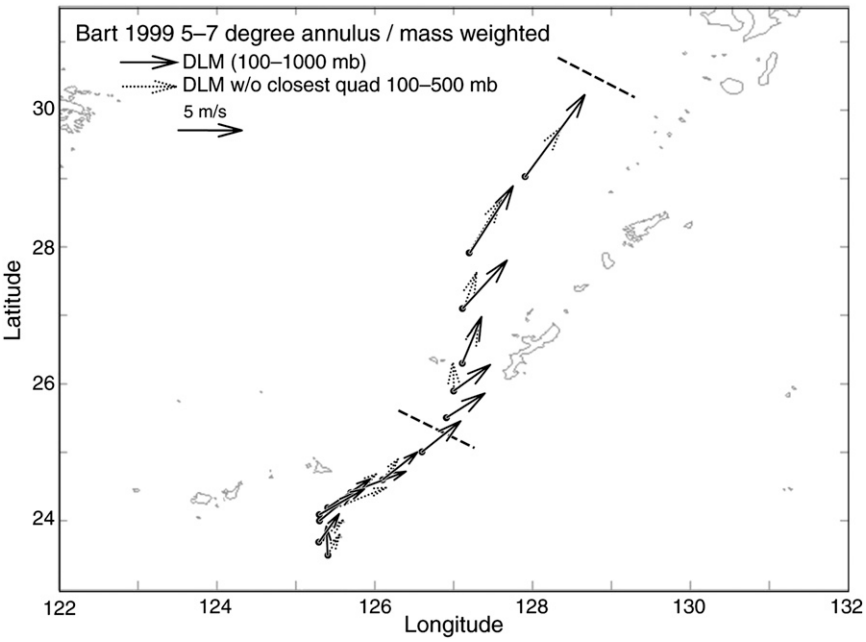


FIG. 16. The original 5°–7° radial band mass-weighted DLM (solid) and the new mass-weighted DLM with the upper-layer quadrant closest to the TUTT cell removed (dotted) for Bart. Mean vectors are scaled to the mean speed of the TC, which is equal to the distance between each 6-hourly time step. Dashed vertical lines mark the interaction start (1800 UTC 21 Sep–0000 UTC 22 Sep 1999) and end (between 1200 and 1800 UTC 23 Sep 1999) points of the TUTT cell interaction period.

with an average of ~1370 km and a standard deviation of ~410 km. The average for all cases was essentially the same as Brand's (1970) 1390-km maximum distance for the onset of mutual cyclonic interaction between two TCs. However, three cases (Babs, Rex1, and Bolaven) with evidence of an interaction had separation distances of ~110 to ~310 km greater than this average, likely due to the larger TUTT cell circulation.

Deeper TUTT cell closed circulations yielded to a greater likelihood of TC deviation (Table 2a), specifically down to 400 hPa or lower (except for Bart). Deeper circulations result in a greater influence on the upper layer and, therefore, the TC's DLM winds. Above 200 hPa, the closed circulation of the TUTT cell typically disappears between 150 and 100 hPa due to the presence of a warm core near the tropopause.

The horizontal extent of the TUTT cell's 200-hPa wind field alone (estimated with the outermost closed 10-m isoheight) was less of a factor than its depth. Since the breadth and separation distance between the circulations are interdependent, the TUTT cell circulation must extend to within the TC's steering environment (~7°) in order to influence its motion. TUTT cell winds on the order of ~15 m $s^{-1}$ at each TC interaction start point within ~7° of the TC's center also appeared to be necessary based on our analysis that provided evidence of a TUTT cell influencing TC motion.

TUTT cell intensity near the interaction start points with 200-hPa PV values greater than 2.5 PVUs and $\zeta_r$ values greater than $1.1 \times 10^{-4}$ $s^{-1}$ resulted in cases where evidence of a TC response was found. Fred was the only exception. TC intensity was also a factor with respect to how the TC responded to the TUTT cell's wind field. TCs Rex2 and Babs provided examples of the possible range of responses in TC motion between two TCs under similar environmental conditions but with contrasting intensities.

### e. Outlier cases

Amber provided evidence of a TUTT cell's influence on TC motion, though its TUTT cell characteristics fit into the group that did not typically reflect evidence of an influence on TC motion. The TUTT cell's closed circulation depth was shallow (~300 hPa) and its intensity was weak (200 hPa PV = ~2 PVUs and $\zeta_r$ = $\sim 1 \times 10^{-4}$ $s^{-1}$; see Tables 2a and 2b) compared to the other cases in this study. The shallowness of the TUTT cell was likely overshadowed by the TC's genesis in proximity to the TUTT cell (<~700 km), which allowed the TC to directly feel this weak TUTT cell's

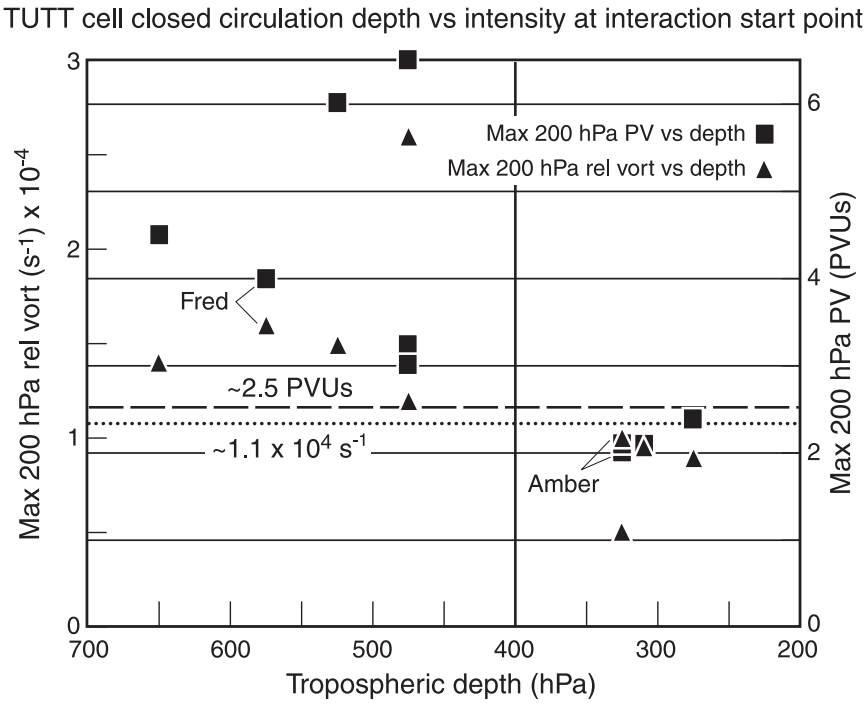


FIG. 17. Maximum depth of the TUTT cell closed circulation near the interaction start point ($x$ axis) vs the (left) 200-hPa intensity in relative vorticity ($y$ axis, $s^{-1}$) and (right) potential vorticity ($y$ axis, PVU; $10^{-6}$ m$^2$ K s$^{-1}$ kg$^{-1}$). Outlier cases are labeled near their two intensity values (aligned vertically). The top-left group yielded evidence of a TUTT cell's influence on TC motion. The bottom-right group did not. The lower limit for cases that provided evidence of a TUTT cell's influence on TC motion is the horizontal dotted line for relative vorticity and the dashed line for potential vorticity.

influence. Even though it had a shallow circulation, the TUTT cell winds were able to extend close to the TC's inner-core circulation (versus its outer 5°–7° environment) and add a northward component to the TC's slow motion.

Contrary to Amber, Fred was accompanied by a very deep and intense TUTT cell but at a relatively large separation distance (~1600 km). The TUTT cell had an expansive wind field at 200 hPa (Table 2c) but narrowed quickly with descending height and rarely reached to within 5° of the TC's center. The TUTT cell did not influence enough of the TC's surrounding upper layer to yield an identifiable response. Rather, synoptic analysis suggested a large stationary anticyclone to Fred's north, at times merging with the TUTT cell's flow on its eastern periphery, which was responsible for Fred's westward motion and an ~18 h southward deviation.

### *f. An Atlantic TC comparison: Hurricane Erin (1995)*

Hurricane Erin was believed to have interacted with ''an upper-level low'' in early August (Rappaport 2006). The hurricane developed over the Bahamas and tracked west-northwestward from 31 July to 3 August (Fig. 18). Around 0000 UTC 1 August, the TC deviated northwestward for 12–18 h, which defined the interaction period. The TUTT cell (called so since the upper-level low originated near 24°N, 45°W, within the Atlantic's midoceanic trough, or TUTT) was generally tracking southwestward ahead of the category 1 (~33 m s$^{-1}$) TC.

Compared to the 10 Pacific cases (Tables 2a and 2b), the TUTT cell was of ''moderate'' intensity with a maximum 200-hPa PV of ~3.7 PVUs, a maximum relative vorticity of $\zeta_r$ of $\sim 1.2 \times 10^{-4}$ s$^{-1}$, and a moderately deep (~400 hPa) and broad (~650 km) closed circulation near the interaction start point. The separation distance during the period decreased quickly from ~650 to ~370 km. The orientation of the two circulations was expected to add a cross-track (to the right or northward) component to the TC's motion with some acceleration late in the interaction (''right/fast'' in Fig. 2).

NHC forecasts called for a straight-line track toward the west-northwest through 48 h for every 6-hourly issuance from 0000 UTC 31 July to 0000 UTC 2 August (not shown). No change in forecast philosophy (e.g., a track deviation) occurred prior to or during the interaction

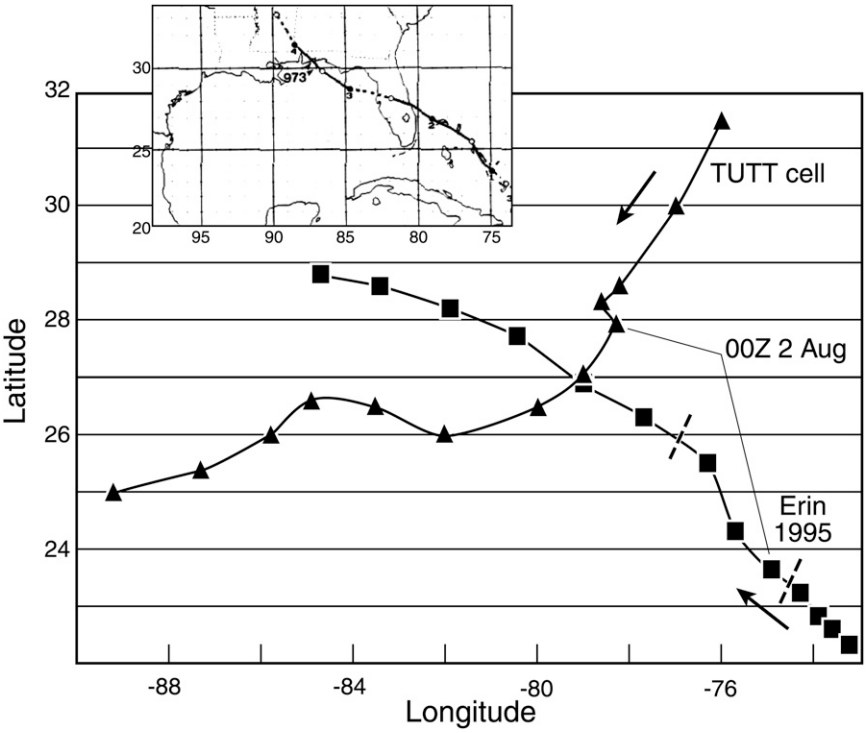


FIG. 18. As in Fig. 3 but for Hurricane Erin (1995) and with the (top left) NHC inset. The dotted lines indicate the estimated start (between 1800 UTC 31 Jul and 0000 UTC 1 Aug 1995) and end (1200–1800 UTC 1 Aug 1995) points of the TUTT cell interaction period.

period. Two dynamic forecast models, the National Centers for Environmental Prediction (NCEP) Global Forecast System and that of the Geophysical Fluid Dynamics Laboratory (GFDL), produced similar forecast tracks. The GFDL, however, did accurately forecast a slight northward track deviation. CLIPER, meanwhile, indicated a gradual recurve scenario toward the north.

A time series of the four layers clearly indicated a northward component of the upper-layer flow within the 1°–3° and 3°–5° radial bands throughout and for 6–12 h on either side of the interaction period. The lower layer did not contribute to the northward bias whatsoever. The 5°–7° upper layer displayed weak and/or southward steering as it incorporates some of the TUTT cell's distant southward return flow while the lower layer maintained a motion vector close to that of the TC motion. Overall, this showed the upper layer (within 5°) was a significant factor in the TC's unexpected northward deviation.

Both the NW (1°–3° radial band) *and* NE (1°–3° and 3°–5° radial bands) quadrants were the main/primary contributors to the mean upper-layer winds. The quadrants were both dominated by TUTT cell flow due to the circulation's proximity. The SE and SW quadrants in all radial bands, meanwhile, remained comparatively negligible.

Figure 19 shows a time series of the original mass-weighted DLM vector and the new DLM vectors with the upper-layer quadrant closest to the TUTT cell removed. A clear influence by the TUTT cell is evident within the two inner radial bands of the new DLM. They both show reduced wind speed magnitudes (~10%–20%) compared to the original DLM vectors but, more significantly, reveal a direction consistently 30°–55° to the left (westward) during the interaction period. The 5°–7° radial band of the new DLM (not shown), meanwhile, remained close to the original DLM in both direction and magnitude. The results fit our model expectations and add credence to the NHC's postanalysis claim.

### g. *Frequency of occurrence*

During the period of this study, the JTWC ATCR documented 169 TCs at tropical storm (17 m $s^{-1}$) or greater intensity for an average of ~5 days each in the northwest Pacific Ocean basin. Initially, 25 TCs had a TUTT cell within 2000 km at some point, though only 9 TCs (2 cases were from Rex) were used due to our case study criteria. Considering the 4.5 days that include the time before, during, and after the interaction period, TUTT cells interact with TCs ~13% of the time in the northwest Pacific Ocean basin.

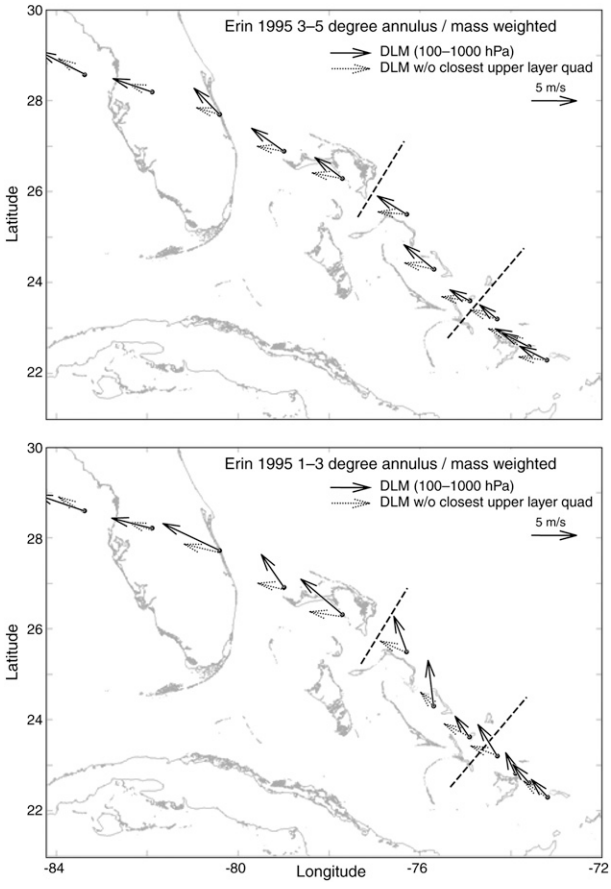


FIG. 19. The original (top) 3°–5° and (bottom) 1°–3° mass-weighted DLM radial band (solid) and the new mass-weighted DLM with the upper-layer quadrant closest to the TUTT cell removed (dotted) for Erin. Mean vectors are scaled to the mean speed of the TC, which is equal to the distance between each 6-hourly time step. Dashed vertical lines mark the interaction start (1800 UTC 31 Jul–0000 UTC 1 Aug 1995) and end points (1200–1800 UTC 1 Aug 1995).

## 4. Conceptual model and conclusions

Figure 20 is a graphical representation of our conceptual model guidance for the influence of a TUTT cell on TC motion designed for operational use at the JTWC. On the left side of Fig. 20, five scenarios provide possible orientations for forecaster pattern recognition. The graphic was designed for forecasters as a ''quick check'' to be applied during each forecast cycle, as needed. This method is similar to Carr and Elsberry's (1994) systematic approach to TC forecasting design. Six yes–no questions provide initial quantified decision-grade criteria to determine if an interaction between the two circulations is likely. These questions, based on our results, are listed below:

1) Is the 200-hPa TUTT cell center within 1700 km (~15°) of the TC?
2) Is the TC and TUTT cell separation distance decreasing?
3) Is the TUTT cell's 200-hPa winds field (>15 m $s^{-1}$) within 800 km (~7°) of the TC's center?
4) Has the TUTT cell maintained a maximum 200-hPa intensity of either
   (a) potential vorticity ≥2.5 PVU or
   (b) relative vorticity ≥11 × $10^{-5}$ $s^{-1}$?
5) Has the TUTT cell maintained a closed circulation at or below 400 hPa?
6) Is the TC at tropical storm intensity or greater?

Six ''yes'' answers indicate a strong likelihood the TUTT cell will exert a predictable influence on TC motion. If *any* answers are ''no,'' an interaction is unlikely at that time. If an interaction is likely, the forecaster can then select a scenario that fits the current situation based on a typical envelope of forecast models referred to as the model ensemble field–trapezoid (e.g., a multimodel ensemble array). The envelope in each scenario is color coded with areas of likely and unlikely [green (annotated with a G) and red (R), respectively] speed and directional biases in the TC's forecast track. The bias is to be applied *after* ensemble forecast track development.

The preliminary scenarios for the conceptual model were derived from the orientation of the circulations within the case studies. Realistic scenarios that did not occur within our cases were inferred. Some scenarios are much less likely to occur and were not included, such as a southward-tracking TC. A TUTT cell located south of a westward-moving TC is another unlikely scenario. Westward-moving TCs are typically south of the subtropical ridge, at low latitudes and south of the TUTT's climatological position. Forecast characteristics of both circulations (orientation, intensity, and separation distance) must be taken into account for continued use of the conceptual model. If the orientation of the two circulations matches one scenario at first but is expected to change to another over time, so must the application of the track bias.

The suggested use of persistence is also provided. Once an interaction is recognized to have begun, persistence should be more heavily weighed (out 12–24 h) during the first 24 h of an identified interaction period. After 24 h, persistence should remain heavily weighed but only for the first 6–12 h since the environment is likely to change in the near future. A change would normally be due to the dissipation of the TUTT cell, an increase in the separation distance between the two circulations, a change in the TC intensity, and/or a change in its orientation. At this point, more forecast weight would return to the traditional model ensemble forecast.

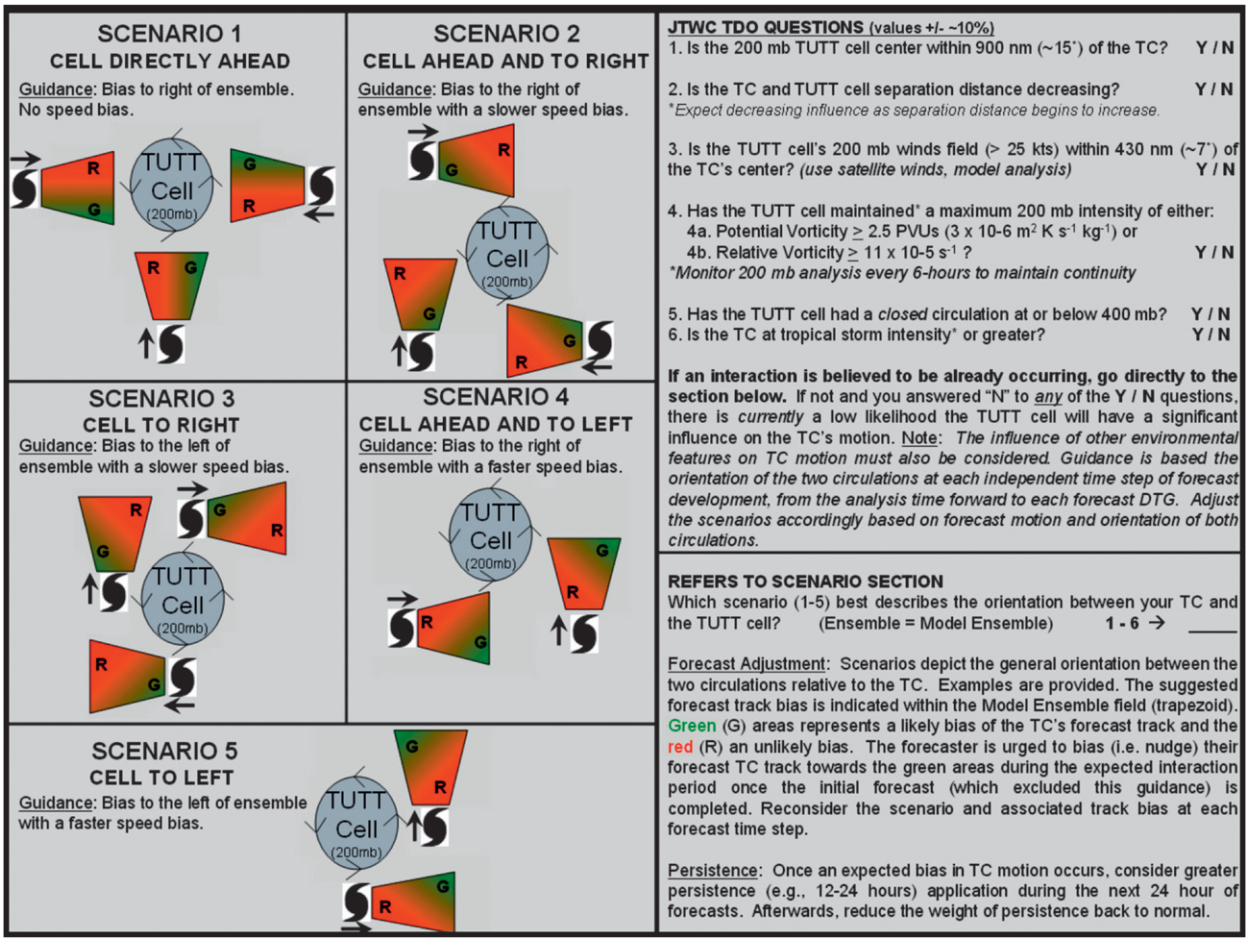


FIG. 20. Conceptual model designed for *operational* guidance at the JTWC. The forecaster initially analyzes the available fields, answers the questions to the upper right in units used by forecasters, and decides whether an interaction is likely. If likely, the forecaster then identifies a similar scenario and applies the recommended TC track and persistence biases. The influence of other TC environmental features must also be incorporated into the decision-making process.

Our research explored a previously undocumented but often referenced topic. We provided evidence, by the use of observational case studies, that TUTT cells do play a significant role in TC motion by affecting a TC's environmental steering flow. Cases in our study demonstrated the link based on our analysis of the TC's environmental flow within specific layers, radial bands, and quadrants of the TC's upper-layer environment. The direction of the bias is based on the orientation of the two circulations and the TUTT cell's downwind flow through the quadrant(s) of the TC closest to the TUTT cell.

Until operational forecast model capability improves, the application of our operational guidance will help to decrease TC forecast track errors during these events. Future similar studies in other basins are warranted to validate the universality of this model or determine its geographical dependency. By the writing of this paper, the guidance had already been reviewed and partially applied at the JTWC. The guidance is also planned to be coordinated at the Central Pacific Hurricane Center (CPHC). The broad nature of the guidance is necessary since only 10 cases are initially used from the Pacific and 1 from the Atlantic.

*Acknowledgments.* This study has been supported by the U.S. Air Force Institute of Technology and NSF Award ATM-0735867. We thank three anonymous reviewers for their helpful suggestions.

## REFERENCES

Brand, S., 1970: Interaction of binary tropical cyclones of the western North Pacific Ocean. *J. Appl. Meteor.,* **9,** 433–441.

Carr, L. E., and R. L. Elsberry, 1990: Observational evidence for predictions of tropical cyclone propagation relative to environmental steering. *J. Atmos. Sci.,* **47,** 542–548.

——, and ——, 1994: Systematic and integrated approach to tropical cyclone track forecasting. Part I: Approach overview and description of meteorological basis. Naval Postgraduate School Tech. Rep. NPS-MR-94-002, Monterey, CA, 273 pp. [Available from Naval Postgraduate School, Monterey, CA 93943-5114.]

——, and ——, 1998: Objective diagnosis of binary tropical cyclone interactions for the western North Pacific basin. *Mon. Wea. Rev.,* **126,** 1734–1740.

——, and ——, 2000a: Dynamical tropical cyclone track forecast errors. Part I: Tropical region error sources. *Wea. Forecasting,* **15,** 641–661.

——, and ——, 2000b: Dynamical tropical cyclone track forecast errors. Part II: Midlatitude circulation influences. *Wea. Forecasting,* **15,** 662–681.

Chan, J. C., and W. Gray, 1982: Tropical cyclone movement and surrounding flow relationships. *Mon. Wea. Rev.,* **110,** 1354–1374.

Chen, G., and L. F. Chou, 1994: An investigation of cold vortices in the upper troposphere over the western North Pacific during the warm season. *Mon. Wea. Rev.,* **122,** 1436–1448.

Colton, D. E., 1973: Barotropic scale interactions in the tropical upper troposphere during the northern summer. *J. Atmos. Sci.,* **30,** 1287–1302.

Dong, K., and C. J. Neumann, 1983: On the relative motion of binary tropical cyclones. *Mon. Wea. Rev.,* **111,** 945–953.

——, and ——, 1986: The relationship between tropical cyclone motion and environmental geostrophic flows. *Mon. Wea. Rev.,* **114,** 115–122.

Elsberry, R. L., 1995: Tropical cyclone motion. *Global Perspectives on Tropical Cyclones,* R. L. Elsberry, Ed., WMO/TD-No. 693, World Meteorological Organization, 106–197.

Fiorino, M., and R. L. Elsberry, 1989: Some aspects of vortex structure related to tropical cyclone motion. *J. Atmos. Sci.,* **46,** 975–990.

Fitzpatrick, P. J., J. A. Knaff, C. W. Landsea, and S. V. Finley, 1995: Documentation of a systematic bias in the Aviation Model's forecast of the Atlantic tropical upper-tropospheric trough: Implications for tropical cyclone forecasting. *Wea. Forecasting,* **10,** 433–446.

Franklin, J. L., 2006: 2005 National Hurricane Center forecast verification report. NOAA/NWS/NCEP/Tropical Prediction Center, 52 pp.

Fujiwhara, S., 1923: On the growth and decay of vortical systems. *Quart. J. Roy. Meteor. Soc.,* **49,** 75–104.

George, J. E., and W. M. Gray, 1976: Tropical cyclone motion and surrounding parameter relationships. *J. Appl. Meteor.,* **15,** 1252–1264.

Glickman, T. S., Ed., 2000: Glossary of Meteorology. *2d ed. Amer. Meteor. Soc.,* 855 pp.

Hogan, T. F., M. S. Peng, J. A. Ridout, and W. M. Clune, 2002: A description of the impact of changes to NOGAPS convection parameterization and the increase in resolution to T239L30. NRL Memo. Rep. NRL/MR/7530-02-52, 10 pp.

Holland, G. J., 1983: Tropical cyclone motion: Environmental interaction plus a beta effect. *J. Atmos. Sci.,* **40,** 328–342.

——, and M. Lander, 1993: The meandering nature of tropical cyclone tracks. *J. Atmos. Sci.,* **50,** 1254–1266.

JTWC, 1994: Annual tropical cyclone report. U.S. Naval Oceanography Command Center, Guam, Mariana Islands, 108 pp. [Available online at http://metocph.nmci.navy.mil/jtwc/atcr/atcr_archive.html.]

——, 1996: Annual tropical cyclone report. U.S. Naval Oceanography Command Center, Guam, Mariana Islands, 101 pp. [Available online at http://metocph.nmci.navy.mil/jtwc/atcr/atcr_archive.html.]

——, 1998: Annual tropical cyclone report. U.S. Naval Oceanography Command Center, Guam, Mariana Islands, 62 pp. [Available online at http://metocph.nmci.navy.mil/jtwc/atcr/atcr_archive.html.]

——, 1999: Annual tropical cyclone report. U.S. Naval Oceanography Command Center, Guam, Mariana Islands, 63 pp. [Available online at http://metocph.nmci.navy.mil/jtwc/atcr/atcr_archive.html.]

Kelly, W. E., and D. Mock, 1982: A diagnostic study of upper tropospheric cold lows over the western North Pacific. *Mon. Wea. Rev.,* **110,** 471–480.

Lander, M. A., and G. J. Holland, 1993: On the interaction of tropical-cyclone-scale vortices. I: Observations. *Quart. J. Roy. Meteor. Soc.,* **119,** 1347–1361.

Neumann, C. J., 1979: On the use of deep-layer-mean geopotential height fields in statistical prediction of tropical cyclone motion. Preprints, *Sixth Conf. on Probability and Statistics in Atmospheric Sciences,* Banff, AB, Canada, Amer. Meteor. Soc., 32–38.

——, 1992: Final report: Joint Typhoon Warning Center (JTWC92) model. SAIC Contract Rep. N 00014-90-C-6042 (Part 2), 83 pp.

Nolan, D. S., Y. Moon, and D. P. Stern, 2007: Tropical cyclone intensification from asymmetric convection: Energetics and efficiency. *J. Atmos. Sci.,* **64,** 3377–3405.

Pike, A., 1985: Geopotential heights and thicknesses as predictors of Atlantic tropical cyclone motion and intensity. *Mon. Wea. Rev.,* **113,** 931–939.

Rappaport, E. N., cited 2006: Preliminary report: Hurricane Erin. Tropical Prediction Center, National Hurricane Center, Miami, FL. [Available online at http://www.nhc.noaa.gov/1995erin.html.]

Sadler, J. C., 1967: The tropical upper tropospheric trough as a secondary source of typhoons and primary source of trade wind disturbances. Hawaii Institute of Geophysics Rep. 67-12, 103 pp.

——, 1975: The upper tropospheric circulation over the global tropics. Dept. of Meteorology Rep. UHMET-75-05, University of Hawaii, Honolulu, HI, 16 pp.

——, 1976: A role of the tropical upper tropospheric trough in early season typhoon development. *Mon. Wea. Rev.,* **104,** 1266–1278.

Sanders, F., and R. W. Burpee, 1968: Experiments in barotropic hurricane track forecasting. *J. Appl. Meteor.,* **7,** 313–323.

Thorncroft, C. D., B. J. Hoskins, and M. E. McIntyre, 1993: Two paradigms of baroclinic-wave lifecycle behavior. *Quart. J. Roy. Meteor. Soc.,* **119,** 17–55.

Velden, C. S., and L. M. Leslie, 1991: The basic relationship between tropical cyclone intensity and the depth of the environmental steering layer in the Australian region. *Wea. Forecasting,* **6,** 244–253.

Whitfield, M. B., and S. W. Lyons, 1992: An upper-tropospheric low over Texas during summer. *Wea. Forecasting,* **7,** 89–106.

Wu, C.-C., and Y. Kurihara, 1996: A numerical study of the feedback mechanisms of hurricane environment interaction of hurricane movement from the potential vorticity perspective. *J. Atmos. Sci.,* **53,** 2264–2282.